IEEE Access
Multidisciplinary | Rapid Review | Open Access Journal

Received February 16, 2021, accepted March 3, 2021, date of publication March 12, 2021, date of current version March 22, 2021.

Digital Object Identifier 10.1109/ACCESS.2021.3065741

Solution Representation Learning in Multi-Objective Transfer Evolutionary Optimization

RAY LIM[1,4], LEI ZHOU[1], ABHISHEK GUPTA[2,4], (Senior Member, IEEE), YEW-SOON ONG[1,2,3], (Fellow, IEEE), AND ALLAN N. ZHANG[4]

[1]School of Computer Science and Engineering, Nanyang Technological University, Singapore 639798
[2]Data Science and Artificial Intelligence Research Centre, Nanyang Technological University, Singapore 639798
[3]Singtel Cognitive and Artificial Intelligence Lab for Enterprises, Nanyang Technological University, Singapore 639798
[4]Singapore Institute of Manufacturing Technology, Agency for Science, Technology and Research (A*STAR), Singapore 138634

Corresponding author: Lei Zhou (lei.zhou@ntu.edu.sg)

This work was supported in part by the Agency for Science, Technology and Research (A*STAR) of Singapore, through the Singapore Institute of Manufacturing Technology-Nanyang Technological University Collaborative Research Programme in Complex Systems, and in part by the A*STAR Cyber-Physical Production System (CPPS) – Towards Contextual and Intelligent Response Research Program, through the RIE2020 IAF-PP Grant A19C1a0018.

ABSTRACT This paper presents a first study on *solution representation learning* for inducing greater alignment and hence *positive transfers* between distinct *multi-objective optimization* tasks that bear discrepancies in their original search spaces. We first establish a novel probabilistic model-based multi-objective transfer evolutionary optimization (TrEO) framework with solution representation learning, capable of activating positive transfers while simultaneously curbing the threat of *negative transfers*. In particular, well-aligned solution representations are learned via spatial transformations to handle mismatches in search space dimensionalities between distinct multi-objective problems, as well as to increase the overlap between their optimized search distributions. We then showcase different algorithmic instantiations and case studies of the proposed framework in applications spanning continuous as well as discrete optimization; illustrative examples include multi-objective engineering design and route planning of unmanned aerial vehicles. The experimental results show that our framework helps induce positive transfers by unveiling useful but hidden inter-task relationships, thus bringing about faster search convergence to solutions of high quality in multi-objective TrEO.

INDEX TERMS Transfer evolutionary optimization, solution representation learning, multi-objective optimization, probabilistic model-based search.

I. INTRODUCTION

The human ability to learn is a masterpiece of natural evolution that has yet to be fully duplicated in artificial systems. When presented with a new task, our brain has the natural tendency to retrieve and reuse *knowledge priors* acquired from related experiences, thereby speeding up our problem-solving process [1]. In the modern era of data-driven optimization, fueled by growing amounts of data and seamless information transmission technologies, it is becoming increasingly important for machines to embody the ability to learn from experiences as well, especially when dealing with complex *real-world* problems [2]–[5]. To this end, a recent computational paradigm known as *transfer evolutionary optimization* (TrEO) [6], [7] has emerged to encompass methods that automatically leverage past problem-solving knowledge to boost optimization efficiency. Under the TrEO label, novel *evolutionary algorithms* (EAs) have been designed to incorporate inter-task learning mechanisms, which enable the exploitation of useful information from related tasks [8]–[12].

An increasing number of works are devoted to investigating the effectiveness of TrEO algorithms in a multitude of real-world applications, including last-mile logistics [13], [14], machine learning [15], [16], neuroevolution [9], and complex engineering design [17]–[19], to name just a few. Given the promising results that have

The associate editor coordinating the review of this manuscript and approving it for publication was Hisao Ishibuchi.

been obtained, there is now growing research attention placed on multi-objective TrEO tasks as well [17]–[24]. This trend is ushered by the complexity of *multi-objective problems* (MOPs) and their ubiquity in the real-world, which together incentivize TrEO approaches. However, we note that despite the potential for performance speed-up, the effectiveness of TrEO algorithms in actual practice could be hampered by the occurrence of harmful *negative transfers* or the scarcity of beneficial *positive transfers* [7], [25].

A typical assumption in existing TrEO methods is that the *source* and *target* tasks share significant overlap in the features of their respective search spaces (e.g., dimensionality), as well as the optimum distribution of solutions in those spaces [25]. Consequently, exploiting knowledge from the source task leads to positive transfers which enhance performance in the target search. However, in many applications it is possible that useful inter-task relationships are concealed by *unaligned solution representations* – characterized by (a) a mismatch between source and target dimensionalities, or (b) a lack of overlap between optimized source and target solution distributions, or both; thus causing reduced positive transfers or even increased negative transfers. This concern is especially potent for real-world multi-objective TrEO settings, given the diverse problem characteristics encountered for MOPs.

On one hand, there is a handful of TrEO research exploring ways to increase positive transfers between distinct optimization problems [26]–[28]. A noteworthy example is the autoencoding evolutionary search paradigm with learning across heterogeneous problems [26]. This approach learns linear transformations of solutions in continuous search spaces, showing promising results of transferring the transformed solutions for a range of multi-objective benchmark problems.

On the other hand, there exist other TrEO methods which are dedicated to curbing the occurrence of negative transfers [9], [10], [20], [29]. One prominent approach is the adaptive model-based transfer EA (AMTEA) [9], which has the ability to suppress undesirable negative transfers from dissimilar sources. The AMTEA captures the degree of source-target similarity via the optimal online stacking of their respective (probabilistic) search distribution models [30], and uses this similarity to determine the extent of inter-task knowledge transmission. However, the efficacy of the AMTEA highly depends on the solution representation spaces in which the source and target tasks are defined. Unaligned solution representations can cause the conservative cancellation of potentially beneficial knowledge transfers between otherwise related problems in the probabilistic TrEO setting, as will be further elaborated in Section III-A.

In this paper, we develop the core idea of learning *solution representations* that induce greater alignment and hence positive transfers between distinct multi-objective optimization tasks that bear discrepancies in their original search spaces. In particular, well-aligned solution representations are learned via search space transformations to (a) handle arbitrary mismatch in source-target dimensionalities, as well as to (b) increase the overlap between optimized search distributions of source and target tasks. Moreover, we emphasize the joint effect of activating positive transfer while simultaneously guarding against negative transfer, in order to achieve the desired performance boost in TrEO algorithms. To the best of our knowledge, there is little previous work in the literature on synergizing these dual effects.

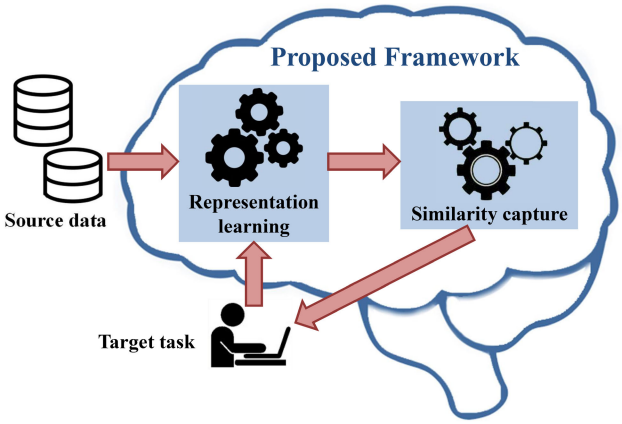

FIGURE 1. An illustration of the proposed TrEO framework that comprises a solution representation learning module to induce positive transfers, as well as a source-target similarity capture mechanism to mitigate negative transfers.

Taking this cue, we establish a novel multi-objective TrEO framework with solution representation learning, synergized with an adaptive probabilistic model-based inter-task similarity capture mechanism to sieve out the threat of negative transfers; Fig. 1 provides an illustration of the proposed framework. Note that the sieving mechanism even serves as a safeguard in cases of inaccurately learned representations, which could be caused by the lack of sufficient target search data required for the training process.

The unique facet of solution representation learning in our framework thus lies in the incorporation of spatial transformation strategies that promise to uncover useful but hidden source-target relationships. In particular, we propose to learn search space mapping functions with the goal of inducing increased positive correlations across performance indicators in multi-dimensional objective space of distinct optimization tasks.

The following points summarize the main theoretical and algorithmic contributions of this paper.

- A novel probabilistic model-based multi-objective TrEO framework with solution representation learning is devised to promote positive transfers while simultaneously mitigating negative transfers.
- Different algorithmic instantiations of our framework are proposed in the context of multi-objective continuous optimization tasks as well as a class of combinatorial optimization problems.
- A range of numerical studies are carried out to verify the efficacy of our methods. The achieved performance advantage is demonstrated not only for complex

benchmark functions, but also for practical examples in vehicle crashworthiness design and in the route planning of unmanned aerial vehicles.

The remainder of this paper is organized as follows. Section II provides preliminary information about probabilistic model-based TrEO algorithms and multi-objective evolutionary optimization. Section III establishes our proposed probabilistic model-based multi-objective TrEO framework, and describes the key novelty of the solution representation learning module. Thereafter, Section IV and Section V present algorithmic instantiations and numerical case studies of this framework for continuous and combinatorial optimization domains, respectively. Finally, Section VI concludes the paper and points to directions for future research.

II. PRELIMINARIES

In this section, we first discuss a probabilistic model-based view of TrEO. A formal definition of multi-objective optimization and a brief review of multi-objective evolutionary algorithms are presented thereafter.

A. PROBABILISTIC VIEW OF TrEO

From the perspective of probabilistic model-based evolutionary search, an optimization task $\mathcal{T}$ with objective function $f(\boldsymbol{x})$ can be formulated as:

$$\max_{p(\boldsymbol{x})} \int_{\mathcal{X}} f(\boldsymbol{x}) p(\boldsymbol{x}) d\boldsymbol{x}, \tag{1}$$

where $\boldsymbol{x} \in \mathcal{X}$ is a candidate solution vector in search space $\mathcal{X}$, and $p(\boldsymbol{x})$ denotes the underlying probability distribution model of the population. (In Eq. (1), we assume objective function maximization without loss of generality.)

Given the approximate nature of the evolutionary optimization procedure, the search is deemed to have converged satisfactorily near to the global optimum f^* of $\mathcal{T}$ once we successfully identify a search distribution model $p^*(\boldsymbol{x})$ that satisfies:

$$\int_{\mathcal{X}} f(\boldsymbol{x}) p^*(\boldsymbol{x}) d\boldsymbol{x} \geq f^* - \varepsilon, \tag{2}$$

where ε is a positive but small convergence threshold.

Traditional EAs are designed to solve optimization problems from scratch without considering past problem-solving experiences. In contrast, the emerging TrEO paradigm ushers in a novel breed of algorithms that aim to exploit knowledge priors from previously solved source tasks to boost the optimization efficiency of the target task at hand. In what follows, we briefly discuss probabilistic model-based TrEO, which is a representative approach equipped with the salient ability to curb negative influences from dissimilar sources.

Let us assume there to be available $T-1$ source tasks, denoted as $\{\mathcal{T}_1, \mathcal{T}_2, \ldots, \mathcal{T}_{T-1}\}$, and their corresponding set of optimized search distribution models to be $\{p_1^*(\boldsymbol{x}), p_2^*(\boldsymbol{x}), \ldots, p_{T-1}^*(\boldsymbol{x})\}$. Given the above, Eq. (1) for the optimization of a target task $\mathcal{T}_T$ can be reformulated as [7],

$$\max_{w_1, w_2, \ldots, w_T, p_T(x)} \int_{\mathcal{X}} f_T(\boldsymbol{x}) \cdot \left[\sum_{S=1}^{T-1} w_S \cdot p_S^*(\boldsymbol{x}) + w_T \cdot p_T(\boldsymbol{x}) \right] \cdot d\boldsymbol{x}, \tag{3}$$

where $f_T(\boldsymbol{x})$ is the target objective function, $p_T(\boldsymbol{x})$ is the target search distribution model, w_S is the *transfer coefficient* of source $S \in \{1, \ldots, T-1\}$, $\sum_{i=1}^{T} w_i = 1$ and $w_i \geq 0 \forall i \in \{1, \ldots, T\}$.

According to [7], it is assumed that $\mathcal{X}$ now represents a *unified search space* in which all the source and target tasks are defined. As a result, the target mixture model $\left[\sum_{S=1}^{T-1} w_S \cdot p_S^*(\boldsymbol{x}) + w_T \cdot p_T(\boldsymbol{x})\right]$ in Eq. (3) can be built through the optimal stacking of source and target models in the unified space $\mathcal{X}$, which provides the transfer coefficients values. In particular, the transfer coefficients in the t^{th} iteration of a probabilistic model-based TrEO algorithm can be obtained by solving the following out-of-sample log-likelihood maximization program:

$$\max_{w_1, w_2, \ldots, w_T} \sum_{\forall \boldsymbol{x} \in P_T(t)} \log \left(\sum_{S=1}^{T-1} w_S \cdot p_S^*(\boldsymbol{x}) + w_T \cdot p_T(\boldsymbol{x}|t) \right), \tag{4}$$

where $P_T(t)$ and $p_T(\boldsymbol{x}|t)$ are the target population data and the current target search distribution model, respectively, at iteration t. Note that Eq. (4) can be resolved to optimality via the stacked density estimation procedure [30] that utilizes the classical expectation-maximization algorithm.

Probabilistic TrEO progresses by iteratively generating populations of candidate solutions through sampling the built target mixture models. Hence, solving Eq. (4) provides the transfer coefficients w_S that capture the source-target similarity, and subsequently mandates the extent to which the sources influence the target search. A larger w_S suggests that the corresponding source's optimized search distribution $p_S^*(\boldsymbol{x})$ overlaps more significantly with the target population, thus supporting source-to-target knowledge transfers at little threat of any harmful interactions. In contrast, a smaller w_S reflects the dissimilarity in the source and target population distributions, thereby preemptively curtailing the transfer of solutions from the corresponding source task $\mathcal{T}_S$.

Most importantly, the idea behind probabilistic TrEO is that if there exists even a single source, say $\mathcal{T}_{S'} \in \{\mathcal{T}_1, \mathcal{T}_2, \ldots, \mathcal{T}_{T-1}\}$, such that $p_{S'}^*(\boldsymbol{x}) \approx p_T^*(\boldsymbol{x})$ – where $p_T^*(\boldsymbol{x})$ is the (*a priori* unknown) optimized target distribution – then, setting $w_{S'}$ close to 1 and sampling from the resultant mixture model would instantly yield near optimal solutions to the target task $\mathcal{T}_T$. The potential for rapid optimization, given the availability of relevant knowledge priors, thus motivates the TrEO paradigm.

B. MULTI-OBJECTIVE EVOLUTIONARY OPTIMIZATION

The statement of Eq. (1) considered a scalar-valued objective function $f(\boldsymbol{x})$. However, many real-world problems often

involve multiple objectives of interest (that are possibly conflicting), hence giving rise to the field of multi-objective optimization [31]. The optimization of a target task $\mathcal{T}_T$ with m conflicting objectives can be formulated as follows [32]:

$$\max_{\boldsymbol{x}} \boldsymbol{F}_T(\boldsymbol{x}) = \left(f_T^1(\boldsymbol{x}), f_T^2(\boldsymbol{x}), \ldots, f_T^m(\boldsymbol{x})\right), \tag{5}$$

where $\boldsymbol{x} = (x_1, \ldots x_d)$ is a d-dimensional solution vector and $\boldsymbol{F}_T$ is a vector of m target objective functions $f_T^i(\boldsymbol{x}), i \in \{1, \ldots, m\}$.

Conflicting objectives in an MOP can generally not be concurrently optimized, thus introducing trade-offs. For this reason, multi-objective optimizers typically solve for a *set* of alternative solutions that constitute the *Pareto-optimal set*, instead of returning just a single optimal solution. Multi-objective EAs (MOEAs), by virtue of their population-based search strategy, have gained increasing popularity for solving MOPs as they are able to attain a reasonable approximation to the entire Pareto set in a single run. Some of the most widely used MOEAs today include the Pareto dominance-based NSGA-II [33] and SPEA2 [34], the decomposition-based MOEA/D [35], [36], and the preference-based PBEA [37], to name a few.

Just like traditional EAs, most existing MOEAs start their search from scratch without any attempt to exploit potentially useful knowledge priors. The recent emergence of the TrEO paradigm has however seen several novel algorithms applied to boost multi-objective optimization performance, by leveraging knowledge from related problems [9], [10], [20], [26]. Nonetheless, these TrEO works have solely focused either on (a) learning inter-task solution mappings as a bid to increase positive transfers, or on (b) curbing detrimental negative transfers from unrelated sources. An approach to jointly address both issues is sorely lacking in the literature. It is with the aim of filling this gap that we put forward the framework in Section III.

III. PROBABILISTIC MODEL-BASED MULTI-OBJECTIVE TrEO WITH SOLUTION REPRESENTATION LEARNING

A. MOTIVATION

Probabilistic model-based TrEO, as discussed in Section II-A, offers the capability to curb negative transfers by assigning low values of transfer coefficients to dissimilar sources. Note in Eq. (3) that the inter-task similarity capture mechanism works based on the assumption that the source and target solutions and models have been encoded in a unified search space $\mathcal{X}$. However, in practice, the source and target problems may be characterized by search spaces $\mathcal{X}_S$ (with dimensionality d_S) and $\mathcal{X}_T$ (with dimensionality d_T), respectively, that are seemingly unaligned – that is, there is either (a) a mismatch in their dimensionalities (i.e., $d_S \neq d_T$), or (b) a large gap between their respective optimized search distributions (i.e., $p_S^*(\boldsymbol{x}_S) \not\approx p_T^*(\boldsymbol{x}_T)$), or both.

Unaligned solution representations nevertheless do not imply that the tasks are unrelated, as their representations may simply be concealing their true relationships. Consider, for example, objective functions (of distinct tasks) that are negatively correlated, representing a definitive inter-task relationship that could be exploited by a transfer optimizer if appropriately gleaned. However, under such circumstances, the existing probabilistic TrEO algorithms would merely negate the transmission of source priors, leading to the conservative cancellation of knowledge transfers. Hence, in the presence of unaligned solution representations, solely focusing on blocking negative transfers would discount potential positive transfers that are useful for the target search.

With the above in mind, in this paper, we put forward the core idea of learning solution representations that induce greater alignment and hence positive transfers between distinct optimization tasks in TrEO. Moreover, we emphasize the importance of activating positive transfers while jointly mitigating the threat of negative transfers in achieving the desired performance advantage of TrEO algorithms. To this end, we develop a novel probabilistic TrEO approach synergized with solution representation learning.

B. PROBABILISTIC TrEO WITH SOLUTION REPRESENTATION LEARNING

In our approach, we realize the solution representation learning through source-to-target mapping functions, denoted hereafter as M_S, which map any source solution $\boldsymbol{x}_S \in \mathcal{X}_S$ from its original search space $\mathcal{X}_S$ to the target search space $\mathcal{X}_T$. In this setup, the source-to-target spatial transformations are learned with the specific aim of achieving well-aligned solution representations (detailed instantiations will be discussed in Section IV and Section V). With this crucial enhancement, probabilistic TrEO algorithms will be capable of inducing positive transfers by (a) handling source-target dimensionality mismatch, and (b) increasing the overlap between source and target optimized search distributions, while also reducing negative transfers from unrelated knowledge priors.

In accordance with Eq. (3), the probabilistic model-based TrEO formulation inclusive of the M_S can be restated as:

$$\begin{aligned} \max_{w_1,\ldots,w_T,p_T(\boldsymbol{x}_T)} & \int_{\mathcal{X}_T} f_T(\boldsymbol{x}_T) \\ & \cdot \left[\sum_{S=1}^{T-1} w_S \cdot p_{M_S}^*(\boldsymbol{x}_T)_S + w_T \cdot p_T(\boldsymbol{x}_T)\right] \cdot \mathrm{d}\boldsymbol{x}_T, \\ \text{s.t.,} & \sum_{S=1}^{T-1} w_S + w_T = 1 \quad \text{and } w_S, \\ & w_T \geq 0 \forall S \in \{1, 2, \ldots, T-1\}, \end{aligned} \tag{6}$$

where $\boldsymbol{x}_T \in \mathcal{X}_T$ is a target candidate solution, $M_S : \mathcal{X}_S \rightarrow \mathcal{X}_T$, and $p_{M_S}^*(\boldsymbol{x}_T)$ is the transformation of $p_S^*(\boldsymbol{x}_S)$ under the mapping M_S. The transformed source model $p_{M_S}^*(\boldsymbol{x}_T)$ can be obtained via simple Monte Carlo approximation; the procedure is given as a pseudocode in Algorithm 1.

Likewise, modifying Eq. (4), the transfer coefficients $w_S, \forall S \in \{1, 2, \ldots, T-1\}$ are obtained by solving the

following mathematical program:

$$\max_{w_1,w_2,\ldots,w_T} \sum_{\forall \boldsymbol{x}_T \in P_T(t)} \log\left(\sum_{S=1}^{T-1} w_S \cdot p^*_{M_S}(\boldsymbol{x}_T) + w_T \cdot p_T(\boldsymbol{x}_T|t)\right). \quad (7)$$

We contend that under appropriately constructed mapping functions M_S, sampling the resultant target mixture model $\left[\sum_{S=1}^{T-1} w_S \cdot p^*_{M_S}(\boldsymbol{x}_T) + w_T \cdot p_T(\boldsymbol{x}_T)\right]$ in Eq. (6) is more likely to yield good solutions for the target task $\mathcal{T}_T$ when knowledge transfers occur (i.e., $w_S > 0$). In other words, our approach makes possible the activation of positive transfers through the source-to-target mapping M_S, while simultaneously reducing negative transfers by sampling the optimal mixture model.

Algorithm 1 Transforming the Source Models via Simple Monte Carlo Approximation

Input: Original source models $p^*_S(\boldsymbol{x}_S)$, $\forall S \in \{1,\ldots,T-1\}$
Output: Transformed source models $p^*_{M_S}(\boldsymbol{x}_T)$, $\forall S \in \{1,\ldots,T-1\}$

1. **For** each $p^*_S(\boldsymbol{x}_S)$
2. Sample N solutions $\boldsymbol{x}_S$ in $\mathcal{X}_S$
3. Apply $M_S : \mathcal{X}_S \rightarrow \mathcal{X}_T$ to obtain N transformed source solutions $\boldsymbol{x}_T = M_S(\boldsymbol{x}_S)$
4. Build a probabilistic model of the transformed source solutions to obtain the transformed source model $p^*_{M_S}(\boldsymbol{x}_T)$
5. **End For**

C. THE PROPOSED MULTI-OBJECTIVE TrEO FRAMEWORK

Following from Section III-B, we now put together a novel probabilistic model-based multi-objective TrEO framework with solution representation learning; detailed in Algorithm 2. In our framework, we assume (without loss of generality) the popular NSGA-II [33] to be the base optimizer. Hence, the concepts of non-dominated sorting and crowding distances to evaluate the relative fitness of candidate solutions in multi-dimensional objective spaces are adopted herein. We label the resultant multi-objective TrEO algorithm as the MOTrEO + M_S.

The inputs to Algorithm 2 include m target objective functions $\boldsymbol{F}_T(\boldsymbol{x}_T) = \left(f^1_T(\boldsymbol{x}_T), f^2_T(\boldsymbol{x}_T), \ldots, f^m_T(\boldsymbol{x}_T)\right)$, a database of knowledge priors (data and optimized probabilistic models) drawn from $T-1$ source tasks, and the transfer interval Δ. Given the inputs, the MOTrEO + M_S proceeds as follows. At the start of optimization, a target population P_T $(t = 1)$ of size N is initialized (lines 1–2). The fitness of each solution is evaluated with respect to the target objectives $\boldsymbol{F}_T$ (line 3). Based on their objective values, the relative fitness of candidate solutions is ascertained via non- dominated sorting and crowding distances across all subsequent iterations of the algorithm. During non-transfer iterations, standard crossover and mutation operators are applied on the parent populations $P_T(t)$ to generate the offspring population $C_T(t)$ (lines 5–6).

When the transfer iterations are triggered by the user-defined parameter Δ, the source-to-target mapping M_S is first learned using both the target population data $P_T(t)$ and the knowledge priors extracted from the source database (lines 7–8). The learned M_S is then applied to obtain the transformed source models $p^*_{M_S}(\boldsymbol{x}_T)$ (line 9); see Algorithm 1. Accordingly, the target mixture model comprising each $p^*_{M_S}(\boldsymbol{x}_T)$ and the current target model $p_T(\boldsymbol{x}_T|t)$ is built, followed by the sampling of the mixture model to generate $C_T(t)$ (lines 10–11). The new population $P_T(t+1)$ for the next iteration is selected from the combined populations $P_T(t) \bigcup C_T(t)$, based on an elitist selection strategy (lines 13–15). The entire evolutionary process repeats until the stopping condition is satisfied.

We note that other existing MOEAs can also be implemented into our proposed framework as the base multi-objective optimizer, by simply modifying the evolutionary operators and selection steps. Furthermore, different types of search space transformations can be integrated into the solution representation learning module of our framework. In the subsequent sections, we present two algorithmic instantiations to learn solution representations in the context of continuous and combinatorial optimization, respectively. Computational experiments are also conducted to showcase the efficacy of our methods, using practical case studies in multi-objective engineering design as well as in the route planning of unmanned aerial vehicles.

IV. METHODOLOGY AND CASE STUDIES IN CONTINUOUS OPTIMIZATION

This section first motivates and describes our methodology for learning solution representations in continuous search spaces. The resultant multi-objective TrEO algorithm synergized with the proposed solution representation learning method is then experimentally validated using complex benchmark problems as well as a real-world case study of vehicle crashworthiness design.

A. LEARNING SOLUTION REPRESENTATIONS IN CONTINUOUS SPACES

Consider a TrEO setting in which high quality solutions from a source task of dimensionality d_S are transformed (using a source-to-target mapping M_S), and transferred to a target problem of size d_T. Existing work has shown promising results of learning transformed source solution representations through linear mapping functions [26], [38]. Although such linear transformations work well when $d_T \leq d_S$, the source's optimized search distribution model $p^*_{M_S}(\boldsymbol{x}_T)$ in the linearly transformed space becomes degenerate when $d_T > d_S$ – as $p^*_{M_S}(\boldsymbol{x}_T)$ will be supported only on a lower d_S-dimensional subspace. Notably, the probabilistic mixture model in Eq. (6) can no longer be built given degenerate priors.

To address the aforementioned issue, some simplistic approaches have been proposed in the literature, including padding additional variables to the solution representations

Algorithm 2 Multi-Objective TrEO With Solution Representation Learning (MOTrEO + $\boldsymbol{M_S}$)

Input: Source database; $\boldsymbol{F}_T$; Δ

Output: Pareto set and optimized search distribution for $\mathcal{T}_T$

1. Set iteration $t = 1$
2. Initialize a population $P_T\ (t)$of N solutions in $\mathcal{X}_T$
3. Evaluate each $\boldsymbol{x}_T$ in $P_T\ (t)$ w.r.t. $\boldsymbol{F}_T$
4. **While** stopping condition not met **do**
5. **If** $mod(t, \Delta) \neq 0$ **then**
6. Generate offspring population $C_T\ (t)$ from $P_T\ (t)$ using recombination and mutation operators
7. **Else**
8. Learn $M_S : \mathcal{X}_S \rightarrow \mathcal{X}_T, \forall S \in \{1, 2, \ldots, T-1\}$ using $P_T\ (t)$ and knowledge priors from the source database
9. Update each $p^*_{M_S}\ (\boldsymbol{x}_T)$ using the corresponding M_S; refer to Algorithm 1
10. Obtain $w_1, w_2, \ldots, w_T$ by solving Eq. (7), then build the target mixture model using all $p^*_{M_S}\ (\boldsymbol{x}_T)$ and $p_T(\boldsymbol{x}_T|t)$
11. Sample the mixture model to obtain offspring $C_T\ (t)$
12. **End If**
13. Evaluate each $\boldsymbol{x}_T$ in $C_T\ (t)$ w.r.t. $\boldsymbol{F}_T$
14. Elitist selection of top N solutions from $P_T\ (t) \bigcup C_T\ (t)$ based on non-dominated sorting and crowding distances, to form $P_T\ (t+1)$
15. Set $t = t + 1$
16. **End While**

[26] or probabilistic models [9] of the source task. However, in many cases of unaligned solution representations (e.g., $p^*_S(\boldsymbol{x}_S) \not\approx p^*_T(\boldsymbol{x}_T)$), these simple approaches are unlikely to suffice in unveiling beneficial inter-task relationships; thereby reducing the potential for positive transfers. In order to handle arbitrary mismatch between source and target dimensionalities (i.e., $d_T > d_S$ and $d_T \leq d_S$) as well as to increase the overlap between their optimized search distributions, we thus propose the source-to-target mapping function M_S as a fast *non-linear* spatial transformation. Under the proposed non-linear mapping, the transformed source model $p^*_{M_S}\ (\boldsymbol{x}_T)$ will not be degenerate even when $d_T > d_S$; hence, making possible the activation of positive inter-task transfers.

Our proposed non-linear mapping function M_S takes the form of a two-layer feedforward neural network:

$$M_S\ (\boldsymbol{x}_S; \boldsymbol{\theta}) = \boldsymbol{\psi}_2\left(\boldsymbol{\psi}_1\ (\boldsymbol{x}_S)\right), \tag{8}$$

where $\boldsymbol{\theta}$ represents the neural network parameters, while $\boldsymbol{\psi}_1$ and $\boldsymbol{\psi}_2$ are the first and second layer transformations, respectively.

In our approach, the mapping M_S is learned using the target and source population data at designated knowledge transfer iterations. Taking motivation from [26], we assume that the source data $P_S(t) = \{\boldsymbol{x}_{S,1}, \ldots, \boldsymbol{x}_{S,N}\}$ of population size N had been archived at every iteration t of an MOEA, when solving the source task $\mathcal{T}_S$ of dimensionality d_S. Further, we adopt the preference relationship between solutions based on the concepts of nondominated front (NF) and crowding distance (CD) that are lexicographically considered in a multi-objective optimization setting [33]; given the common knowledge of these terms in the associated literature, we refrain from providing a detailed discussion about them herein for the sake of brevity. Accordingly, a solution $\boldsymbol{x}_1$ is preferred over another solution $\boldsymbol{x}_2$ if any one of the following conditions holds true [39]: (i) $\text{NF}_1 < \text{NF}_2$ or (ii) $\text{NF}_1 = \text{NF}_2$ and $\text{CD}_1 > \text{CD}_2$; see Fig. 2(a). This preference relationship shall be assumed hereafter for evaluating and ranking solutions in $P_S(t)$ as well as in the target population (as was also done in Algorithm 2).

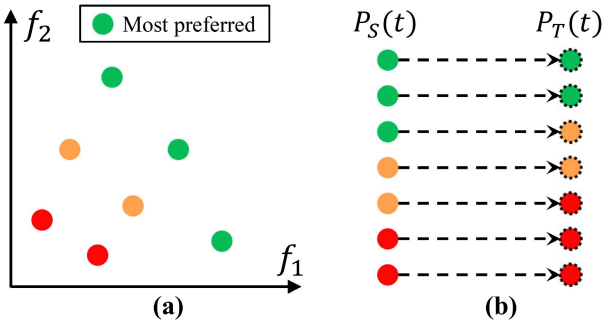

FIGURE 2. (a) The preference relationship between solutions in a multi-objective setting (assuming objective function maximization). (b) Source and target populations monotonically aligned according to decreasing order of preference.

In the optimization of a target task $\mathcal{T}_T$ of dimensionality d_T, let the target population data at iteration t be $P_T(t) = \{\boldsymbol{x}_{T,1}, \ldots, \boldsymbol{x}_{T,N}\}$. A necessary step for learning a mapping M_S between $P_S(t)$ and $P_T(t)$ is to first *sort* the solutions in both $P_S(t)$ and $P_T(t)$ according to the preference relationship defined above. This induces a monotonic alignment between the source and target population sets, as shown in Fig. 2(b). Preferred solutions in the source data are matched with those in the target data, and vice versa, thereby facilitating the discovery of source-to-target mappings that tend to induce a high ordinal correlation (on the preference relationship scale) across tasks in the transformed solution representation space. Assuming the Pareto sets of the source and target tasks to be located in the regime (i.e., not far from the underlying distribution) of $P_S(t)$ and $P_T(t)$, respectively, transforming optimal solutions of the source with M_S could then help generate optimal solutions to the target as well.

Given the motivation and data alignment procedure above, the M_S in Eq. (8) is learned through the following two-layer transformations:

$$\boldsymbol{\psi}_1\ (\boldsymbol{x}_S) = \sigma\ (\boldsymbol{A}_1 \cdot \boldsymbol{x}_S + \boldsymbol{b}), \tag{9}$$

and,

$$M_S = \boldsymbol{\psi}_2\left(\boldsymbol{\psi}_1\ (\boldsymbol{x}_S)\right) = \boldsymbol{A}_2 \cdot \boldsymbol{\psi}_1\ (\boldsymbol{x}_S), \tag{10}$$

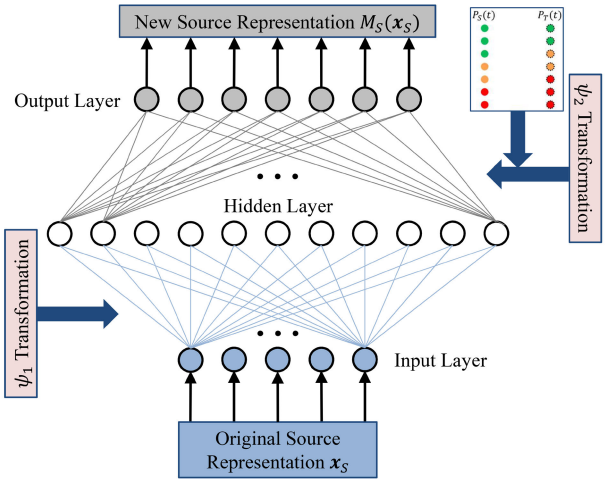

FIGURE 3. An illustration of the methodology to learn solution representations in continuous spaces, using a two-layer feedforward neural network.

where matrices $\boldsymbol{A}_1 \in \mathbb{R}^{d_h \times d_S}$ and $\boldsymbol{A}_2 \in \mathbb{R}^{d_T \times d_h}$ contain the neural network's weighting terms, $\boldsymbol{b}$ is a bias vector, and σ is the non-linear sigmoidal activation function; d_h represents the number of neurons in the hidden layer.

In the spirit of [40] supporting fast learning, we randomly assign and then fix the elements of $\boldsymbol{A}_1$ in Eq. (9). Thereafter, the elements of $\boldsymbol{A}_2$ in Eq. (10) are obtained using the following closed-form expression:

$$\boldsymbol{A}_2 = P_T \cdot \left[\boldsymbol{\psi}_1(P_s)\right]^{\mathrm{tr}} \cdot \left(\boldsymbol{\psi}_1(P_s) \cdot \left[\boldsymbol{\psi}_1(P_s)\right]^{\mathrm{tr}} + \lambda \cdot I_{d_h}\right)^{-1}, \tag{11}$$

where $[\cdot]^{\mathrm{tr}}$ symbolizes a matrix transpose, I_{d_h} is an identity matrix of size d_h, and λ is the L_2 regularization coefficient of network parameters. Fig. 3 gives an illustration of the solution representation learning via the proposed M_S.

In accordance with Eq. (6), the learned M_S is applied to the source model $p_s^*(\boldsymbol{x}_s)$ to obtain the transformed source model $p_{M_S}^*(\boldsymbol{x}_T)$ via simple Monte Carlo approximation; refer to Algorithm 1. In our implementation for continuous optimization problems, the $p_{M_S}^*(\boldsymbol{x}_T)$ and the current target model $p_T(\boldsymbol{x}_T|t)$ are actualized as multi-variate Gaussian distributions. The target and transformed source models are then used in the stacked density estimation procedure [30] to build the mixture model $[\sum_{S=1}^{T-1} w_S \cdot p_{M_S}^*(\boldsymbol{x}_T) + w_T \cdot p_T(\boldsymbol{x}_T|t)]$ in the target search space $\mathcal{X}_T$; see Eq. (6).

With reference to our multi-objective TrEO framework (Algorithm 2) in Section III, the proposed mapping M_S forms the key component of the solution representation learning module, while the resultant multi-objective TrEO algorithm is similarly labeled as the MOTrEO + M_S. In the following sub-sections, the performance advantage of our algorithm is experimentally verified.

B. AN EXAMPLE OF COMPLEX MULTI-OBJECTIVE BENCHMARKS

Here we first showcase the effectiveness of the MOTrEO+M_S using complex multi-objective benchmark problems characterized by varying degree of discrepancies between the source and target tasks [41].

TABLE 1. Experimental results for the multi-objective benchmark tasks after 50,000 function evaluations. In bold are the best results (values with 95% confidence level based on the Wilcoxon signed-rank test are marked with "∗"). Results are reported based on 20 independent runs of all optimizers.

Problem Configuration	Average IGD Values			
	NSGA-II	NSGA-II $+M_S$	AMTEA	MOTrEO $+M_S$
CIHS	0.27	0.29	**0.01**	**0.01**
CIMS	8.01	8.96	**4.45**	4.57
CILS	12.16	13.52	9.41	**8.32**
PIHS	3.02	3.84	2.48	**2.46**
PIMS	243.22	126.34	74.76	**26.43***
PILS	20.37	20.14	20.23	**1.04***
NIHS	100.02	97.51	87.97	**84.44**
NIMS	8.78	7.19	7.36	**3.33***
NILS	20.30	20.29	20.31	**7.11***

1) EXPERIMENTAL SPECIFICATIONS

Table 1 (leftmost column) shows the problem configuration of nine multi-objective TrEO tasks considered in this study. The source and target dimensionalities are set to $d_S = 10$ and $d_T = 20$, respectively. The four-letter problem configuration represents the known degree of discrepancies between the source and target tasks (i.e., $\mathcal{T}_S$ and $\mathcal{T}_T$, respectively). Each configuration comprises the extent of *intersection* (overlap) between the Pareto sets of $\mathcal{T}_S$ and $\mathcal{T}_T$, as well as a degree of *similarity* between the fitness landscapes of $\mathcal{T}_S$ and $\mathcal{T}_T$. For instance, we have: (i) CIHS:*complete* intersection with *high* similarity; (ii) PIMS: *partial* intersection with *medium* similarity; and (iii) NILS: *no* intersection with *low* similarity. Readers are referred to [41] for the full details of these benchmark problems. We expect that a smaller extent of intersection between source-target Pareto optimal solutions (i.e., "no" < "partial" < "complete" intersection), and a lower degree of similarity in the fitness landscapes (i.e., "low" < "medium" < "high" similarity) will increase the scope for the MOTrEO + M_S to unveil useful but hidden inter-task relationships.

Four optimizers[1] are considered for comparison in this example. They are: (i) the base optimizer NSGA-II (without knowledge transfer) [33], (ii) NSGA-II+M_S which is a recently proposed TrEO algorithm [26] adapted using the non-linear mapping function M_S in Section IV-A, (iii) AMTEA which is the state-of-the-art probabilistic model- based TrEO algorithm without solution representation learning [9], and (iv) our proposed MOTrEO+M_S. All search populations of size $N = 50$ consist of real-coded solutions. The optimizers employ simulated binarycrossover, polynomial mutation (with probability $1/d_T$) and tournament

[1]Codes for the implementation of all the considered algorithms are available at www.github.com/raylim-sg/MOTrEO.git

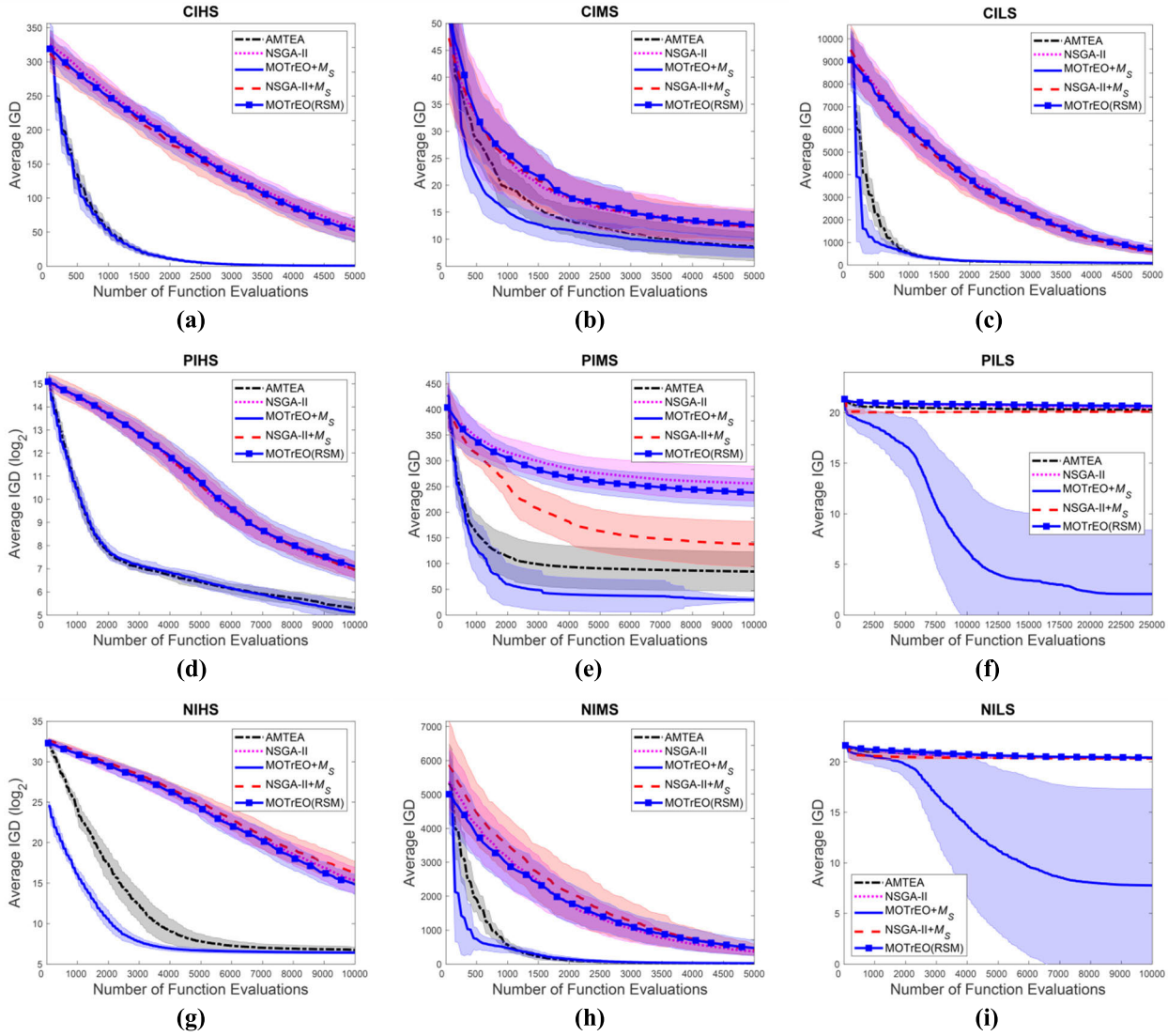

FIGURE 4. Convergence trends for the complex multi-objective benchmark tasks in Table 1. Results are for distinct problem configurations: "high similarity" (leftmost column), "medium similarity" (central column), "low similarity" (rightmost column), "complete intersection" (top row), "partial intersection" (middle row), and "no intersection" (bottom row). The shaded regions span one standard deviation on either side of the mean (based on 20 independent runs).

selection. The transfer interval is set to $\Delta = 2$, at which target mixture models with multi-variate Gaussian components are built and sampled in the AMTEA and the MOTrEO+M_S. For the two-layer neural network in the NSGA-II+M_S^{NL} and the MOTrEO+M_S, we set the number of neurons in the hidden layer to $d_h = 2d_T$. The *inverted generational distance* (IGD) [42] is used as the multi-objective performance indicator to quantify the solution quality returned by all algorithms. A single-run of each algorithm is terminated after 50,000 function evaluations.

2) RESULTS AND DISCUSSION

Table 1 summarizes average IGD values returned by the four optimizers after 20 independent runs. The MOTrEO+M_S has outperformed the other algorithms in 8 out of 9 cases, among which it has achieved significant difference in 4 cases. The convergence trends are illustrated in Fig. 4 for all the cases, while the transfer coefficients patterns are shown in Fig. 5 for three representative cases, namely, CIHS, PILS and NILS. Looking at CIHS, PIHS and NIHS with high inter-task similarity even in the original solution representation spaces, our expectation is closely borne out by the almost equivalent convergence rates between the AMTEA and the MOTrEO+M_S, as well as their comparable transfer coefficients obtained; see Fig. 4(a), (d), (g), and Fig. 5(a). This observation is explained by the high similarities between source and target function landscapes, which leaves little to be gained through learning solution representations in the MOTrEO+M_S.

In contrast, the MOTrEO+M_S significantly outperforms the other algorithms in PIMS, PILS, NIMS and NILS. The results are attributed to the increased degree of discrepancies between the source and target tasks in those cases, giving rise

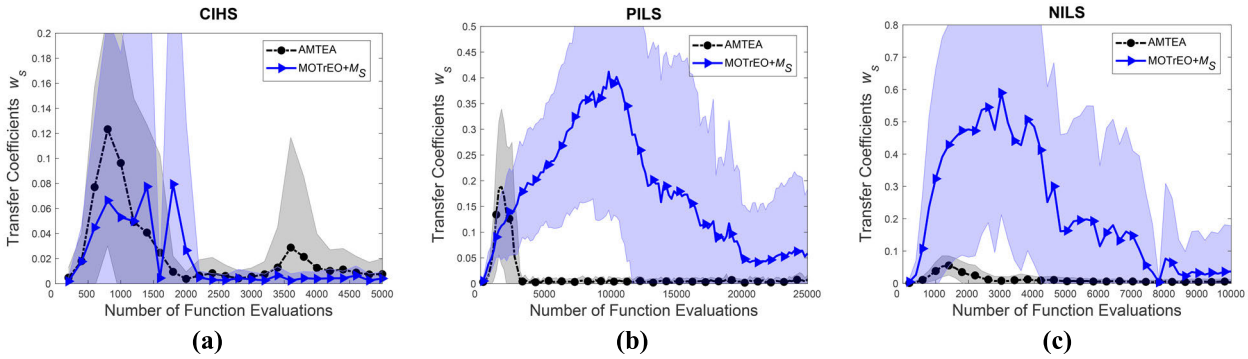

FIGURE 5. The transfer coefficients learned by the AMTEA and the MOTrEO + M_S in three cases. (a) CIHS. (b) PILS. (c) NILS.

to the scope for solution representation learning to unveil hidden source-target relationships. Moreover, the multimodality of the target tasks in PILS and NILS increases their difficulty substantially, which further incentivizes the solution representation learning in the MOTrEO+M_S. The performance advantage of our algorithm is clearly manifested in its significantly higher convergence rates and transfer coefficients obtained; see Fig. 4(f), (i) and Fig. 5(b), (c), respectively.

Positive transfers are empirically identified when an algorithm's convergence rate is boosted. Hence, we can say that the MOTrEO+M_S's performance advantage is attributed to the presence of positive transfers, which in turn imply larger transfer coefficients. The theoretical developments in [9] in fact show that the learning of transfer coefficients in probability mixture model-based search explicitly reduces negative inter-task interactions, relative to the no-transfer case. Take PILS and NILS as examples. We observe that the MOTrEO+M_S's enhanced convergence rates are accompanied by larger transfer coefficients, whereas the AMTEA's slower convergence is accompanied by near-zero transfer coefficients; as shown in Fig. 4 and Fig 5. For NILS in particular, the synergistic effect of activating positive transfers while jointly mitigating the threat of negative transfers is demonstrated in Fig. 6, where larger transfer coefficients are obtained only when the learned mapping M_S is effective. In a nutshell, observing both (a) an enhanced convergence rate, and (b) larger transfer coefficients obtained, are good indicators of the target search benefitting from positive transfers from the available sources.

To further affirm that the effectiveness of the MOTrEO+M_S is indeed by virtue of positive transfers induced by the source-to-target mapping M_S (and is not a spurious artifact of introducing diversity through knowledge transfers from external sources), we consider an additional MOEA that transfers the solutions sampled from a *random source model* (RSM), which we label as the MOTrEO(RSM). The RSM takes the form of a *uniform distribution defined over the search space*, which is solely intended for introducing diversity into the target population. It is worth noting that in the MOTrEO(RSM), the amount of knowledge transfers is determined by the transfer coefficients obtained in the MOTrEO+M_S, which

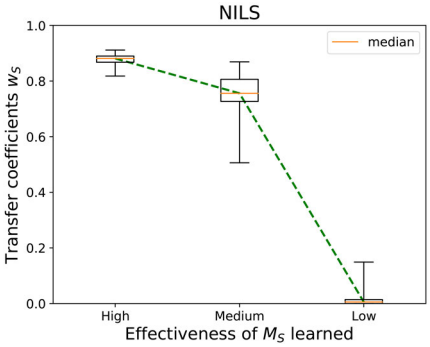

FIGURE 6. The transfer coefficients derived in the MOTrEO + M_S are large only when the learned mapping is effective in inducing positive transfers. The effectiveness of M_S learned is measured by the average Euclidean distance between the transformed source solutions and their corresponding nearest target Pareto optimal solution. For instance, the effectiveness of M_S is considered to be "high", "medium" or "low" when the distances are "< 0.3", "0.3 – 0.5" or "> 0.5", respectively.

ensures that both algorithms receive the same extent of solution transfers from external sources. Results show that the convergence trends of the MOTrEO(RSM) are only comparable to those of the NSGA-II (without knowledge transfers) for all the problem configurations, which are consistently worse than those of the MOTrEO+M_S; see Fig. 4. Therefore, the efficacy of our proposed algorithm in inducing positive transfers across tasks is verified in the experimental results.

C. A PRACTICAL CASE IN VEHICLE CRASHWORTHINESS DESIGN

Following from the promising results for benchmark MOPs, we now demonstrate the effectiveness of the MOTrEO+M_S in a real-world application of vehicle crashworthiness design.

Crashworthiness is an important quality of vehicle designs that aims to reduce human injury in the event of collision impact. The vehicle crashworthiness design optimization is often a computationally expensive problem that involves multiple objectives. In this case study, we consider the minimization of three critical objectives, namely, the vehicle mass, the jerk, and the vehicle toeboard intrusion. Readers

can refer to [43] for the mathematical model and a detailed description of this design problem.

Here, the multi-objective minimization program can be simply stated as:

$$\begin{aligned} &\min\ F(\boldsymbol{x}) = (f_{mass}(\boldsymbol{x}), f_{jerk}(\boldsymbol{x}), f_{intrusion}(\boldsymbol{x})), \\ &\text{s.t.,}\ \boldsymbol{x} = (x_1, \ldots, x_d)^{\mathrm{T}} \quad and\ 1mm \leq x_j \leq 3mm,\ \forall j, \end{aligned} \tag{12}$$

where $f_{mass}(\boldsymbol{x}), f_{jerk}(\boldsymbol{x})$ and $f_{intrusion}(\boldsymbol{x})$ are the objective functions for vehicle mass, jerk and toeboard intrusion, respectively, $\boldsymbol{x}$ is a candidate solution vector, d is the number of design variables and x_j refers to the j^{th} design variable.

In real-world settings, it is possible that the source and target tasks bear arbitrary discrepancies in their respective search spaces. For instance, (a) having different number of design variables (i.e., $d_S \neq d_T$), and (b) lacking one-to-one alignment between source and target design variables – we refer to this scenario as $\mu_S \neq \mu_T$; take for example, $\boldsymbol{x}_S = (x_3, x_1, x_2)^{\mathrm{T}}$ and $\boldsymbol{x}_T = (x_1, x_2, x_3, x_4, x_5)^{\mathrm{T}}$. Such misalignments generally reduce the overlap of optimized search distributions between the source and target problems, which could lead to reduced positive transfers or even increased negative transfers.

Despite the presence of the aforementioned discrepancies, we contend that our proposed algorithm, by virtue of automatically learning well-aligned solution representations, is able to uncover useful inter-task relationships and induce positive transfers. To verify this, we conduct experiments using distinct cases of the problem in Eq. (12) characterized by arbitrary source-target discrepancies as described above.

1) EXPERIMENTAL SETUP

We consider three multi-source transfer scenarios as follows: (i) Case 1: $d_T = d_{S1}, d_T = d_{S2}$ and $\mu_T \neq \mu_{S1}, \mu_T \neq \mu_{S2}$, (ii) Case 2: $d_T > d_{S1}, d_T > d_{S2}$ and $\mu_T = \mu_{S1}, \mu_T \neq \mu_{S2}$, and (iii) Case 3: $d_T = d_{S1}, d_T > d_{S2}$ and $\mu_T \neq \mu_{S1}, \mu_T \neq \mu_{S2}$. The same four optimizers as Section IV-B are considered for comparison. The population size in this case study is set to $N = 15$ [43]. A single run of each algorithm is terminated after 300 function evaluations. The average IGD values are computed based on 20 independent runs, using the Pareto front which is approximated beforehand with 20,000 function evaluations of all the four optimization algorithms under comparison.

2) RESULTS AND DISCUSSION

Table 2 gives a summary of the experimental results that are averaged over 20 independent runs for all the three cases. The highlight of Table 2 is that the MOTrEO+M_S consistently performs better than the other algorithms in terms of solution quality and speed. Equipped with both the solution representation learning module as well as the source-target similarity capture mechanism, our algorithm achieves performance enhancement through a favorable balance between the activation of positive transfers and the concurrent reduction of negative transfers. In contrast, without any source induced search bias, the base (non-TrEO) NSGA-II is consistently outperformed by the other optimizers.

TABLE 2. Results for the multi-objective vehicle crashworthiness design tasks after 300 function evaluations. In bold Are the best results (values with 95% confidence level based on the Wilcoxon signed-rank test Are marked with "∗"). Results Are reported based on 20 independent runs of all optimizers.

Problem Configuration	Average IGD Values			
	NSGA-II	NSGA-II +M_S	AMTEA	MOTrEO +M_S
$d_T = d_{S1}, d_T = d_{S2}$ and $\mu_T \neq \mu_{S1}, \mu_T \neq \mu_{S2}$	0.415	0.403	0.411	**0.373**∗
$d_T > d_{S1}, d_T > d_{S2}$ and $\mu_T = \mu_{S1}, \mu_T \neq \mu_{S2}$	0.415	0.377	0.386	**0.361**
$d_T = d_{S1}, d_T > d_{S2}$ and $\mu_T \neq \mu_{S1}, \mu_T \neq \mu_{S2}$	0.415	0.400	0.401	**0.359**∗

Comparing the AMTEA and the MOTrEO+M_S in Table 2, relative to the NSGA-II, the AMTEA shows smaller improvements in solution quality. The presence of unaligned source-target solution representations in each case substantiates the scope for our proposed solution representation learning method to unveil hidden source-target relationships. The superiority of our algorithm is manifested in its higher convergence rates and larger transfer coefficients obtained; see Fig. 7(a), (b), (c) and Fig. 7(d), (e), (f), respectively. What is more, despite executing the same solution representation learning module, the MOTrEO+M_S outperforms the NSGA-II+M_S in all cases. The NSGA-II+M_S is not equipped with the probabilistic model-based inter-task similarity capture mechanism, thereby failing to adaptively control the extent of knowledge transfers from the various sources to the target task.

The numerical results of this case study confirm the efficacy of our proposed MOTrEO+M_S in inducing positive transfers between distinct real-world MOPs defined in continuous search spaces. However, we note that other than continuous optimization problems, there exists a plethora of real-world applications of MOPs in domains of discrete and combinatorial optimization. This brings us to the next section where a novel algorithmic instantiation of solution representation learning in multi-objective TrEO is proposed for a class of combinatorial vehicle routing tasks.

V. A METHODOLOGY AND CASE STUDY IN COMBINATORIAL VEHICLE ROUTING PROBLEMS

In this section, we first consider a practical TrEO scenario in which the multi-objective route planning of unmanned aerial vehicles benefit from past experiences of optimizing ground-based *vehicle routing problems* (VRPs). We then highlight the importance of solution representation alignment in the effectiveness of knowledge transfers between distinct VRPs. To this end, we propose a novel methodology

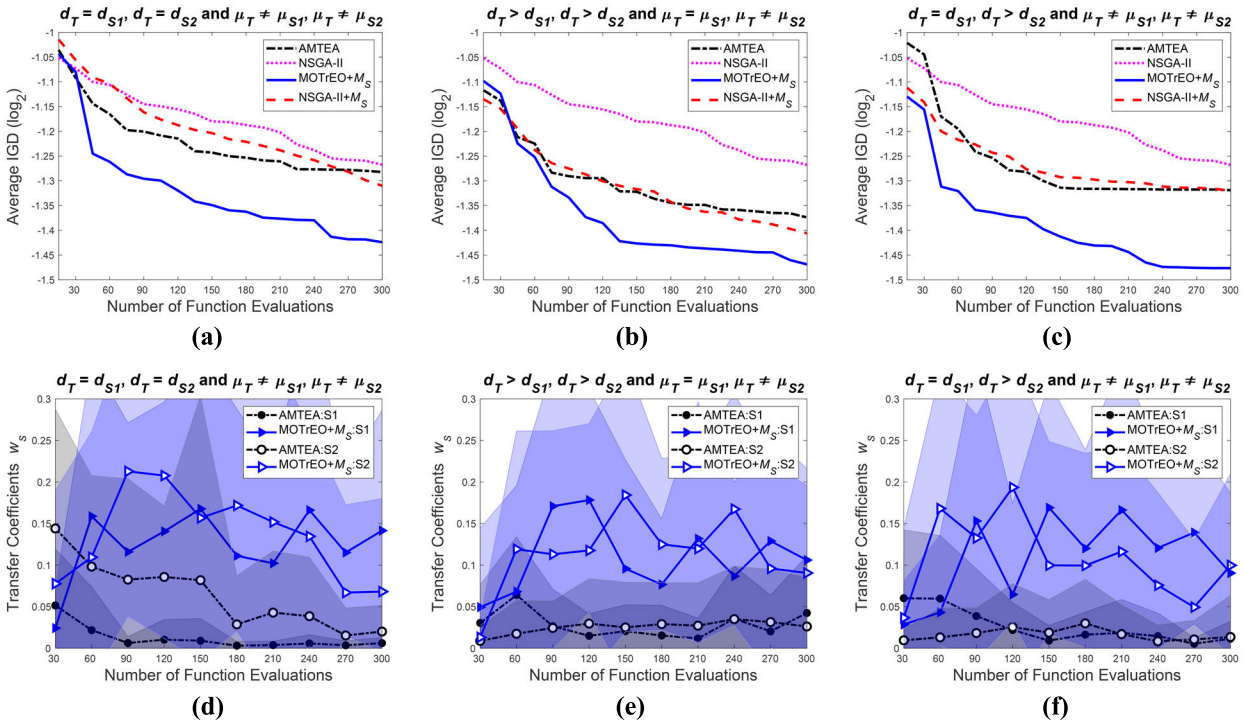

FIGURE 7. Convergence trends for the target multi-objective vehicle crashworthiness design optimization task and the transfer coefficients learned by the AMTEA and the MOTrEO + M_S in *Case 1*: $d_T = d_{S1}$, $d_T = d_{S2}$ and $\mu_T \neq \mu_{S1}$, $\mu_T \neq \mu_{S2}$ (left column), *Case 2*: $d_T > d_{S1}$, $d_T > d_{S2}$ and $\mu_T = \mu_{S1}$, $\mu_T \neq \mu_{S2}$ (central column), and *Case 3*: $d_T = d_{S1}$, $d_T > d_{S2}$ and $\mu_T \neq \mu_{S1}$, $\mu_T \neq \mu_{S2}$ (rightmost column).

to learn well-aligned solution representations via source-to-target spatial transformations, with the aim of unveiling beneficial inter-task structural similarities. Computational experiments are conducted to verify that our method can effectively utilize knowledge priors from previously optimized ground-based VRPs, to speed up the optimization tasks of multi-objective route planning of unmanned aerial vehicles.

A. A MULTI-OBJECTIVE LAST-MILE LOGISTICS EXEMPLAR

Recent years have seen the growing use of unmanned aerial vehicles (e.g., drones) as an alternative to ground vehicles (e.g., trucks) for last-mile delivery, as drones can be deployed more swiftly at lower operating costs. Drone delivery route planning commonly minimizes multiple objectives such as the total distance travelled and the number of drones needed to satisfy customer demands [44]. For the above reasons, it is important to rapidly optimize multi-objective drone delivery problems under essential operational requirements. Here we put forward a TrEO case study that aims to boost the multi-objective optimization efficiency of drone delivery planning tasks, by exploiting knowledge priors from related ground-based VRPs.

We note that it is common practice to solve drone delivery tasks as 2-D variants of ground-based VRPs [44]. This is due to similar problem characteristics involved, such as minimizing the total route distance under the constraints of capacity and travel distance limits. In view of the aforesaid, we choose the well-studied truck delivery route planning problems as the source tasks in this study. Our choice is further motivated by the abundance of past problem-solving experiences accumulated in the domain of truck delivery planning [45]. The following formalizes the source and target tasks for our case study.

1) TRUCK DELIVERY (SOURCE) PROBLEM

We define the source task on an undirected graph $G = (V, E)$, where $V = \{v_i\}$ is the set of vertices (i.e., customer nodes) and $E = \{e_{ij}\}$ is the set of edges connecting vertices v_i and v_j, for $i, j = 1, \ldots, d_S$, while d_S is the number of customers. The single depot is represented by vertex v_0 which stations K number of trucks. The vehicles are allowed to do multiple trips that start and end at the depot, and they are constrained by delivery capacity Q and maximum travel distance limit L per trip. Each customer i has a known deterministic demand $c_{S,i}$ and a distance $z_{S,i}$ from the depot. They are served by vehicle k in route r, where $k = 1, \ldots, K$ and $r = 1, \ldots, R$. Let $D_{k,r}$ be the distance travelled and $W_{k,r}$ be the weight capacity served by vehicle k in route r. The objective and constraint functions are then formulated as follows:

$$\min f_S = \sum_{r=1}^{R} \cdot \sum_{k=1}^{K} D_{k,r},$$
$$s.t.,\ D_{k,r} \leq L \quad and\ W_{k,r} \leq Q,\ \forall k,\ \forall r, \qquad (13)$$

where f_S is the source objective function to minimize the total truck distance travelled after serving all customer demands.

2) MULTI-OBJECTIVE DRONE DELIVERY (TARGET) PROBLEM

We define the target task on an undirected graph $H = (U, A)$, where $U = \{u_i$ is the set of vertices and $A = \{a_{ij}\}$ is the set of edges connecting vertices u_i and u_j, for $i, j = 1, \ldots, d_T$, such that d_T is the number of customer nodes. The single depot is represented by vertex u_0, at which each drone starts and ends a route b. All the drones have a delivery capacity q, a maximum travel distance l per route and a maximum flight range from the depot h. Any customer j has a known deterministic demand $c_{T,j}$ and a distance $z_{T,j}$ from the depot. They can only be served once by a drone y in route b, where $y, b = 1, \ldots, B$. We assume that the drones are not allowed to do multiple trips due to their limited power capacity that requires time-consuming battery recharging. As such, a total of B number of drones is needed to complete B number of routes. Further, let $D_{y,b}$ be the distance travelled and $W_{y,b}$ be the payload served by drone y in route b. We formulate the objective and constraint functions as follows:

$$\begin{aligned} &\min_{\boldsymbol{x}_T} \ \boldsymbol{F}(\boldsymbol{x}_T) = \left(f_T^1(\boldsymbol{x}_T), f_T^2(\boldsymbol{x}_T)\right), \\ &s.t., \ f_T^1 = B, \quad f_T^2 = \sum_{y,b}^{B} D_{y,b}, \\ &\qquad q \ll Q, \quad l \ll L, \ W_{y,b} \leq q, \ D_{y,b} \leq l \ and \\ &\qquad z_{T,j} \leq h, \quad \forall y, \ \forall b, \ \forall j, \end{aligned} \tag{14}$$

where $\boldsymbol{x}_T$ is a target candidate solution, f_T^1 and f_T^2 are the target objective functions to minimize the number of drones and the total flight distance, respectively. Eq. (14) accounts for the essential operating constraints of real commercial drones including smaller payload, shorter flight distance per route and limited flight range from the depot [46].

B. LEARNING SOLUTION REPRESENTATIONS IN PERMUTATION-BASED COMBINATORIAL SPACES

One of the most widely used solution representations in VRPs is the *permutation* of customer node indices to determine the order of visiting the customers. *This permutation-based representation is dependent on the index number assigned to each customer node, as well as the geometric distribution of nodes*. Furthermore, we note that different real-world vehicle routing tasks are likely to have different customer node indices and distributions, despite possibly sharing structurally similar optimal routes or sub-routes. This is likely to give rise to unaligned solution representations between distinct routing tasks, which could in turn reduce the effectiveness of TrEO.

To illustrate, consider the optimal routes of distinct source and target vehicle routing tasks as seen in Fig. 8. The routes could be encoded as permutation-based solution representations, such as [0, 1, 2, 3, 4, 0, 5, 6, 7, 8, 0, 9, 10, 11, 12, 0] and [0, 1, 5, 0, 4, 6, 8, 3, 0, 9, 2, 7] for the source and target VRPs, respectively [47]. Fig. 8 entails some structural overlaps of source-target optimal sub-routes, which can be identified by the coloured customer nodes. Despite the existence of such overlaps, the source and target solution representations appear to be completely different because of the arbitrary indices assigned to their customer nodes. This suggests that directly sampling and transferring solutions from the source instance in Fig. 8(a) to the target instance in Fig. 8(b) is unlikely to result in positive transfers, or it may even cause negative transfers. Following from the above, it is clear that the solution representation alignment is crucial to the success of knowledge transfers between VRPs.

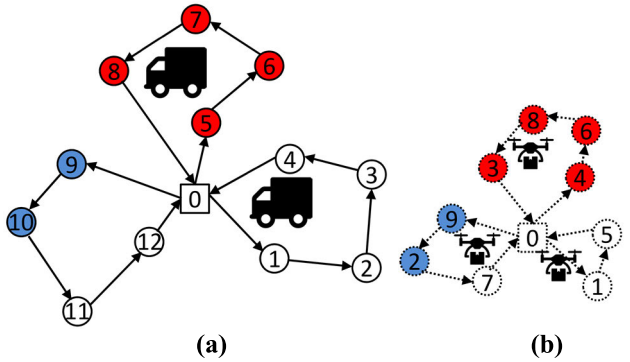

FIGURE 8. The importance of solution representation alignment in the effectiveness of knowledge transfers between two distinct vehicle routing tasks, featuring the overlap of their optimal sub-routes. (a) The known optimal routes of source graph *G*. (b) The (a priori unknown) optimal routes of target graph *H*.

With that in mind, we propose a novel methodology to learn well-aligned solution representations in permutation-based combinatorial spaces, with the aim of inducing positive transfers between distinct vehicle routing tasks. Specifically, our method produces new source representations via a *two-step strategy* as follows.

Step 1: A source-to-target mapping, denoted as M_S, is first constructed to match as closely as possible, the source and target problems' geometric distributions of customer nodes. Under the mapping function M_S, the source graph is first scaled to a geometric size that is comparable with the target. The source is then translated and rotated to align the centroid and principal components of its customer distribution with those of the target graph. The overall source-to-target spatial transformation through M_S is mathematically defined as:

$$\begin{aligned} M_S(\boldsymbol{x}_{S,i}) &= \alpha \boldsymbol{A} \cdot \boldsymbol{x}_{S,i} + \boldsymbol{b}, \quad \forall i, \\ \text{s.t., } \alpha &= \frac{\sum_{j=1}^{d_T} z_{T,j}/d_T}{\sum_{i=1}^{d_S} z_{S,i}/d_S}, \\ \boldsymbol{A} &= \begin{bmatrix} cos\theta & -sin\theta \\ sin\theta & -cos\theta \end{bmatrix}, \end{aligned} \tag{15}$$

where $\boldsymbol{x}_{S,i} \in \mathbb{R}^{2\times 1}$ is the Cartesian coordinates vector of a source node $i \in \{1, \ldots, d_S\}$, $\alpha \in \mathbb{R}^{\mathcal{C}}$ is a scaling constant, $\boldsymbol{A}$ is an angular rotation matrix, θ is the angle between the principal components of the source and target graphs, and $\boldsymbol{b} \in \mathbb{R}^{2\times 1}$ is a translation vector.

Step 2: Reassign the index numbers of all the source nodes by copying the indices from the corresponding nearest target nodes. If the source has more nodes than the target (i.e., $d_S > d_T$), randomly assign a number $i \in \{1, \ldots, d_S\}$ without replacement to the remaining $(d_S - d_T)$ nodes. The new source representation is thus learned.

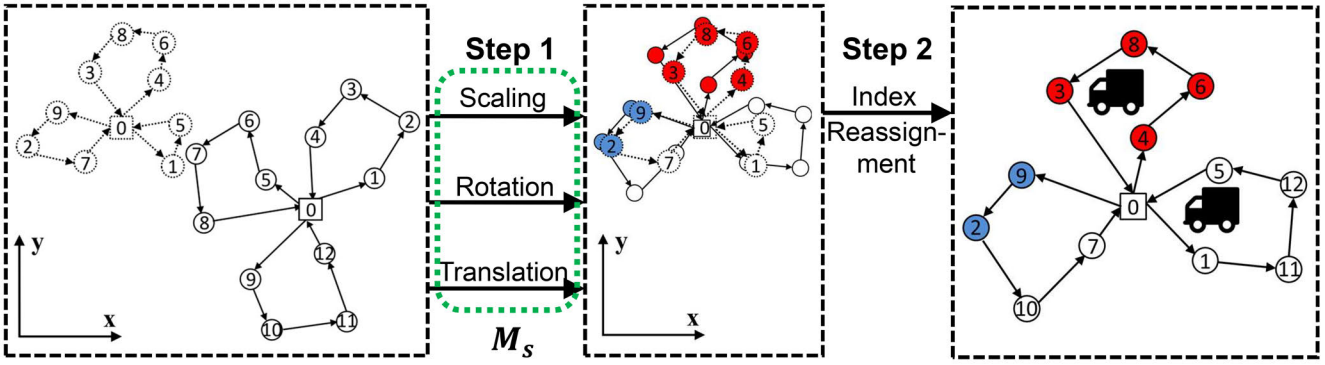

FIGURE 9. A graphical illustration of the proposed methodology to learn well-aligned solution representations for distinct VRPs. (a) The original source and target graphs. (b) The source-to-target transformation M_S in Step 1. (c) The source node index reassignments in Step 2.

Our proposed method is based on the intuition that the transformations in Eq. (15) of Step 1, together with Step 2, will lead to a closer alignment of customer nodes indices and distributions between the source and target VRPs. As a consequence, the learned source solution representations will be more likely to capture any overlap of optimal routes or sub-routes between the source and target tasks. Fig. 9 illustrates the solution representation learning via our proposed approach. Given the original source and target graphs in Fig. 9(a) that may appear to lack transferrable sub-routes, the M_S in Step 1 attempts to match their geometric distribution of customer nodes as shown in Fig. 9(b). Step 2 of our approach is depicted in Fig. 9(b), (c), where each source node is assigned a new index number based on the geometrically nearest target node.

Besides, it is worth noting that the mapping M_S in Eq. (15) preserves shortest paths, hence our method does not change the optimal routes of the source in the transformed space. This is proven in *Lemma 1* below.

Lemma 1: The source-to-target transformations in Eq. (15) preserve the source problem's original graph structure and shortest paths.

Proof: Firstly, the angular rotation, translation and compression of a graph are rigid transformations that lead to direct isometry. Secondly, the linear combination of isometries is also an isometry. Since isometry preserves geometric structure [48], it is hence proven that the M_S in Eq. (15) preserves the source task's original graph structure and shortest paths.

Here, we similarly label the resultant multi-objective TrEO algorithm with the proposed solution representation learning methodology as the MOTrEO+M_S. The following computational experiments serve to verify the efficacy of our algorithm in boosting the performance of the target multi-objective optimization task of drone delivery route planning defined in Eq. (14).

C. EXPERIMENTS

1) SOURCE AND TARGET INSTANCES

We generate vehicle routing instances from several existing VRP datasets [49]–[51]. For the truck delivery (source) instances, we either consider the original datasets or modify the datasets by removing an arbitrary number of customer nodes. The dimensionalities of the source and target problems, denoted as d_S and d_T, respectively, are moderately large with up to a few hundred customers. In our implementation, we generate new multi-objective drone delivery (target) instances according to the following procedure: (i) create a new target instance using only the Cartesian coordinates of customer nodes from the original dataset; (ii) arbitrarily transform the geometric distribution of customer nodes and randomly assign an index number to each node; (iii) set the drone travel distance limit $l = 50$, and randomly generate the flight range h between $[5, 10]$ in L_2-norm distances, the payload limit q between $[20, 200]$ in kilograms, as well as the customer demands $c_{T,j}$ between $[1, 5]$ in kilograms, for $j = 1, \ldots, d_T$; (iv) remove customer nodes located beyond the range h. The drone constraints and customer demands values are based on the specifications of real commercial drones.

2) EXPERIMENTAL SETUP

Four optimizers[2] are considered for comparison in this our experiments. They are: (i) the base NSGA-II [33], (ii) a multi-objective variant of the edge histogram-based sampling algorithm (EHBSA) which is a probabilistic model-based optimizer for combinatorial problems [52], (iii) the AMTEA without solution representation learning [9], and (iv) our proposed MOTrEO+M_S. All search populations of size $N = 100$ consist of permutation-coded solutions. Excluding EHBSA, the other algorithms execute optimized crossover (with probability 0.75) along with inversion or swap sequence mutation (with probability 0.2) [53]. For EHBSA, the sampling without template strategy is used with its default parameter settings.

The transfer interval is set to $\Delta = 5$, at which target probabilistic mixture models with edge histogram-based source and target components [52] are built in the AMTEA and the MOTrEO+M_S. During non-transfer search iterations, both AMTEA and MOTrEO+M_S execute NSGA-II as the base

[2]Codes for the implementation of all the considered algorithms are available at www.github.com/raylim-sg/MOTrEO.git

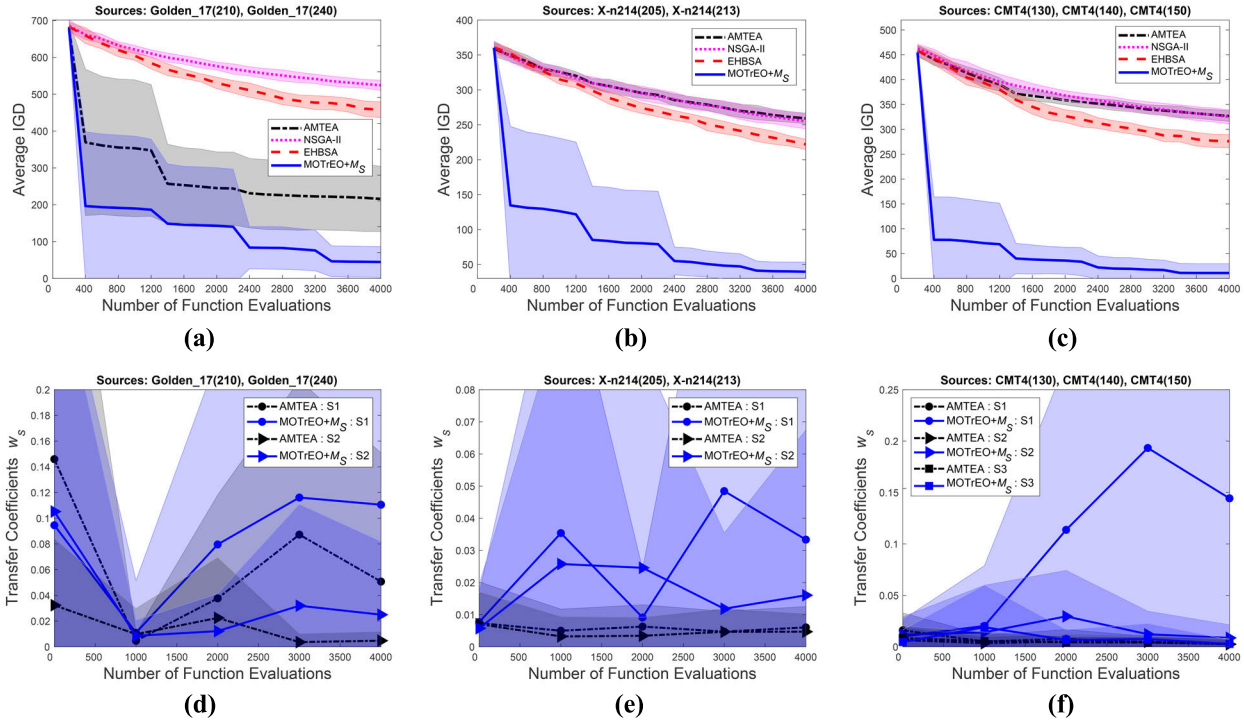

FIGURE 10. **Convergence trends for the target multi-objective optimization task of drone delivery route planning, and the transfer coefficients obtained by the AMTEA and the MOTrEO + M_S, for target instances Golden_17 (left column), X-n214 (central column) and CMT4 (rightmost column). The shaded regions span one standard deviation on either side of the mean (based on 20 independent runs).**

MOEA. The MOTrEO+M_S incorporates the solution representation learning methodology described in Section V-B. The solution quality achieved by all the optimizers is measured using the IGD performance metric [42]. A single-run of each optimizer is terminated after 10,000 function evaluations, whereas the true Pareto front is approximated at the end of 100,000 function evaluations of NSGA-II.

3) RESULTS AND DISCUSSION

The average IGD values achieved by the four optimizers after 20 independent runs are provided in Table 3. Fig. 10 depicts the convergence trends of all the optimizers and the transfer coefficients obtained by the AMTEA and the MOTrEO+M_S, for 3 representative target instances. The highlight of Table 3 is that the MOTrEO+M_S performs significantly better than all the other algorithms for all the six cases. Moreover, the convergence rates of the MOTrEO+M_S are significantly enhanced in the early stages of the optimization processes, as seen in Fig. 10(a), (b), (c). These outcomes are attributed to the activation of positive transfers in our algorithm, made possible by well-aligned solution representations learned through the proposed source-to-target transformation. For example, the larger w_S values learned by the MOTrEO+M_S in Fig. 10(d), (e), (f) show that it is able to uncover beneficial source-target structural overlap, which is exploited to boost the target search. The superior performance of the MOTrEO+M_S is also explained by its ability to achieve a complementary balance between inducing positive transfers and mitigating harmful negative transfers.

TABLE 3. **Experimental results for the target multi-objective drone delivery tasks after 10,000 function evaluations. In bold Are the best results (values with "$*$" achieve 95% confidence level based on the Wilcoxon signed-rank test). Results Are reported based on 20 independent runs of all optimizers.**

Problem Instance	d_s	Average IGD Values			
		NSGA-II	EHBSA	AMTEA	MOTrEO +M_S
M-n151 ($d_T = 144$)	135, 140	175.37	170.63	184.17	**10.38** $*$
X-n214 ($d_T = 200$)	205, 213	130.50	131.45	143.76	**6.38** $*$
Golden_17 ($d_T = 222$)	210, 240	334.22	366.31	127.59	**3.05** $*$
Golden_18 ($d_T = 282$)	290, 300	346.67	308.07	208.09	**70.46** $*$
CMT4 ($d_T = 133$)	130, 140, 150	185.63	211.40	192.00	**0.35** $*$
X-n162 ($d_T = 143$)	140, 150, 161	184.35	173.71	198.44	**57.61** $*$

In contrast, the AMTEA achieves second best performance in 2 out of 6 cases, but it performs the worst in 3 out of 6 cases (i.e., M-n151, X-n214, X-n162). Without the solution representation learning module, the AMTEA's performance is adversely impacted by the extra efforts required to sieve out negative transfers caused by unaligned source-target solution representations. The AMTEA is also less capable of facilitating positive transfers; as reflected by the smaller w_S values obtained in Fig. 10(d), (e), (f). These

observations affirm the efficacy of our method in uncovering useful routes or sub-routes that remain hidden in the original search spaces of source tasks. The proposed MOTrEO+M_S is indeed more effective at leveraging related VRPs to enhance the performance on multi-objective route optimization of unmanned aerial vehicles.

In summary, this case study clearly demonstrates the utility of solution representation learning for inducing positive transfers between distinct but related vehicle routing tasks.

VI. CONCLUSION

This paper is motivated by the core idea of learning solution representations as the means to induce positive transfers in TrEO for multi-objective optimization. Accordingly, we established a probabilistic model-based multi-objective TrEO framework that encompasses a novel solution representation learning module. The framework enables the integration of methodologies to learn spatial transformations, which are aimed at overcoming discrepancies between the original search spaces of source and target tasks. The salient feature of the resultant multi-objective TrEO algorithm is its ability to promote positive transfers through learning well-aligned solution representations that unveil useful but hidden source-target relationships, while simultaneously mitigating the threat of negative transfers.

Following from the proposed framework, we put forward different algorithmic instantiations in the context of multi-objective continuous optimization tasks as well as a class of combinatorial optimization problems. In addition to rigorous comparisons on complex multi-objective optimization benchmarks, we demonstrated the efficacy of our methods in practical case studies of multi-objective engineering design as well as the route planning of unmanned aerial vehicles. The computational results affirmed that our proposed TrEO algorithm was able to increase positive transfers of knowledge priors from available source tasks, which led to enhanced convergence rate and solution quality of the target problem.

In the future, one of our main research directions will be to further expand the applicability of our approach to a wider variety of real-world optimization problems (e.g., simulation-based problems characterized by computationally expensive function evaluations). It would also be interesting to explore ways to improve the utilization efficiency of the available source data.

ACKNOWLEDGMENT

The author Yew-Soon Ong thanks the support by Singtel Cognitive and Artificial Intelligence Lab for Enterprises (SCALE@NTU), which is a collaboration between Singapore Telecommunications Limited (Singtel) and Nanyang Technological University (NTU) that is funded by the Singapore Government through the Industry Alignment Fund – Industry Collaboration Projects Grant.

REFERENCES

[1] T. Ward and A. Plagnol, "Defined by our past," in *Cognitive Psychodynamics as an Integrative Framework in Counselling Psychology and Psychotherapy*. Cham, Switzerland: Palgrave Macmillan, 2019, pp. 69–88.

[2] L. Bai, Y.-S. Ong, T. He, and A. Gupta, "Multi-task gradient descent for multi-task learning," *Memetic Comput.*, vol. 12, no. 4, pp. 355–369, Dec. 2020.

[3] Y. Jin, H. Wang, T. Chugh, D. Guo, and K. Miettinen, "Data-driven evolutionary optimization: An overview and case studies," *IEEE Trans. Evol. Comput.*, vol. 23, no. 3, pp. 442–458, Jun. 2019.

[4] M. Pelikan, M. W. Hauschild, and P. L. Lanzi, "Transfer learning, soft distance-based bias, and the hierarchical BOA," in *Proc. Int. Conf. Parallel Problem Solving Nature (PPSN)*, 2012, pp. 173–183.

[5] M. Iqbal, W. N. Browne, and M. Zhang, "Reusing building blocks of extracted knowledge to solve complex, large-scale Boolean problems," *IEEE Trans. Evol. Comput.*, vol. 18, no. 4, pp. 465–480, Aug. 2014.

[6] A. Gupta, Y.-S. Ong, and L. Feng, "Insights on transfer optimization: Because experience is the best teacher," *IEEE Trans. Emerg. Topics Comput. Intell.*, vol. 2, no. 1, pp. 51–64, Feb. 2018.

[7] A. Gupta and Y. S. Ong, *Memetic Computation: The Mainspring of Knowledge Transfer in a Data-Driven Optimization Era*, vol. 21. Cham, Switzerland: Springer, 2018.

[8] A. Gupta, Y.-S. Ong, and L. Feng, "Multifactorial evolution: Toward evolutionary multitasking," *IEEE Trans. Evol. Comput.*, vol. 20, no. 3, pp. 343–357, Jun. 2016.

[9] B. Da, A. Gupta, and Y.-S. Ong, "Curbing negative influences online for seamless transfer evolutionary optimization," *IEEE Trans. Cybern.*, vol. 49, no. 12, pp. 4365–4378, Dec. 2019.

[10] K. K. Bali, A. Gupta, Y.-S. Ong, and P. S. Tan, "Cognizant multitasking in multiobjective multifactorial evolution: MO-MFEA-II," *IEEE Trans. Cybern.*, early access, Apr. 23, 2020, doi: 10.1109/TCYB.2020.2981733.

[11] Y.-S. Ong and A. Gupta, "AIR5: Five pillars of artificial intelligence research," *IEEE Trans. Emerg. Topics Comput. Intell.*, vol. 3, no. 5, pp. 411–415, Oct. 2019.

[12] C. Lyu, Y. Shi, and L. Sun, "A novel multi-task optimization algorithm based on the brainstorming process," *IEEE Access*, vol. 8, pp. 217134–217149, Dec. 2020.

[13] L. Feng, L. Zhou, A. Gupta, J. Zhong, Z. Zhu, K.-C. Tan, and K. Qin, "Solving generalized vehicle routing problem with occasional drivers via evolutionary multitasking," *IEEE Trans. Cybern.*, early access, Dec. 23, 2019, doi: 10.1109/TCYB.2019.2955599.

[14] J. MacLachlan, Y. Mei, J. Branke, and M. Zhang, "Genetic programming hyper-heuristics with vehicle collaboration for uncertain capacitated arc routing problems," *Evol. Comput.*, vol. 28, no. 4, pp. 563–593, 2020.

[15] Q. U. Ain, H. Al-Sahaf, B. Xue, and M. Zhang, "Generating knowledge-guided discriminative features using genetic programming for melanoma detection," *IEEE Trans. Emerg. Topics Comput. Intell.*, pp. 1–16, 2020.

[16] Y. Bi, B. Xue, and M. Zhang, "An effective feature learning approach using genetic programming with image descriptors for image classification [research frontier]," *IEEE Comput. Intell. Mag.*, vol. 15, no. 2, pp. 65–77, May 2020.

[17] A. T. W. Min, Y.-S. Ong, A. Gupta, and C.-K. Goh, "Multiproblem surrogates: Transfer evolutionary multiobjective optimization of computationally expensive problems," *IEEE Trans. Evol. Comput.*, vol. 23, no. 1, pp. 15–28, Feb. 2019.

[18] C. Yang, J. Ding, Y. Jin, C. Wang, and T. Chai, "Multitasking multiobjective evolutionary operational indices optimization of beneficiation processes," *IEEE Trans. Autom. Sci. Eng.*, vol. 16, no. 3, pp. 1046–1057, Jul. 2019.

[19] Z. Wang and X. Wang, "Multiobjective multifactorial operation optimization for continuous annealing production process," *Ind. Eng. Chem. Res.*, vol. 58, no. 41, pp. 19166–19178, Oct. 2019.

[20] J. Zhang, W. Zhou, X. Chen, W. Yao, and L. Cao, "Multisource selective transfer framework in multiobjective optimization problems," *IEEE Trans. Evol. Comput.*, vol. 24, no. 3, pp. 424–438, Jun. 2020.

[21] C. Yang, J. Ding, Y. Jin, and T. Chai, "Offline data-driven multiobjective optimization: Knowledge transfer between surrogates and generation of final solutions," *IEEE Trans. Evol. Comput.*, vol. 24, no. 3, pp. 409–423, Jun. 2020.

[22] O. R. Castro, A. Pozo, J. A. Lozano, and R. Santana, "Transfer weight functions for injecting problem information in the multi-objective CMA-ES," *Memetic Comput.*, vol. 9, no. 2, pp. 153–180, Jun. 2017.

[23] J. Lin, H. L. Liu, B. Xue, M. Zhang, and F. Gu, "Multiobjective multitasking optimization based on incremental learning," *IEEE Trans. Evol. Comput.*, vol. 24, no. 5, pp. 824–838, Oct. 2020.

[24] H. T. Thanh Binh, N. Quoc Tuan, and D. C. Thanh Long, "A multi-objective multi-factorial evolutionary algorithm with reference-point-based approach," in *Proc. IEEE Congr. Evol. Comput. (CEC)*, Jun. 2019, pp. 2824–2831.

[25] R. Lim, A. Gupta, Y.-S. Ong, L. Feng, and A. N. Zhang, "Non-linear domain adaptation in transfer evolutionary optimization," *Cognit. Comput.*, vol. 13, no. 2, pp. 290–307, Mar. 2021.

[26] L. Feng, Y.-S. Ong, S. Jiang, and A. Gupta, "Autoencoding evolutionary search with learning across heterogeneous problems," *IEEE Trans. Evol. Comput.*, vol. 21, no. 5, pp. 760–772, Oct. 2017.

[27] K. K. Bali, A. Gupta, L. Feng, Y. S. Ong, and T. Puay Siew, "Linearized domain adaptation in evolutionary multitasking," in *Proc. IEEE Congr. Evol. Comput. (CEC)*, Jun. 2017, pp. 1295–1302.

[28] L. Feng, A. Gupta, and Y.-S. Ong, "Compressed representation for higher-level meme space evolution: A case study on big knapsack problems," *Memetic Comput.*, vol. 11, no. 1, pp. 3–17, Mar. 2019.

[29] X. Zheng, A. K. Qin, M. Gong, and D. Zhou, "Self-regulated evolutionary multitask optimization," *IEEE Trans. Evol. Comput.*, vol. 24, no. 1, pp. 16–28, Feb. 2020.

[30] P. Smyth and D. Wolpert, "Stacked density estimation," in *Proc. Adv. NIPS*, Denver, CO, USA, 1998, pp. 668–674.

[31] K. Taha, "Methods that optimize multi-objective problems: A survey and experimental evaluation," *IEEE Access*, vol. 8, pp. 80855–80878, Apr. 2020.

[32] Z. Wang, Y.-S. Ong, and H. Ishibuchi, "On scalable multiobjective test problems with hardly dominated boundaries," *IEEE Trans. Evol. Comput.*, vol. 23, no. 2, pp. 217–231, Apr. 2019.

[33] L. M. Pang, H. Ishibuchi, and K. Shang, "NSGA-II with simple modification works well on a wide variety of many-objective problems," *IEEE Access*, vol. 8, pp. 190240–190250, Oct. 2020.

[34] E. Zitzler, M. Laumanns, and L. Thiele, "SPEA2: Improving the strength Pareto evolutionary algorithm," ETH Zürich, Zürich, Switzerland, TIK-Rep. 103, 2001.

[35] Q. Zhang and H. Li, "MOEA/D: A multiobjective evolutionary algorithm based on decomposition," *IEEE Trans. Evol. Comput.*, vol. 11, no. 6, pp. 712–731, Dec. 2007.

[36] T.-C. Wang, R.-T. Liaw, and C.-K. Ting, "MOEA/D using covariance matrix adaptation evolution strategy for complex multi-objective optimization problems," in *Proc. IEEE Congr. Evol. Comput. (CEC)*, Jul. 2016, pp. 983–990.

[37] K. Li, M. Liao, K. Deb, G. Min, and X. Yao, "Does preference always help? A holistic study on preference-based evolutionary multiobjective optimization using reference points," *IEEE Trans. Evol. Comput.*, vol. 24, no. 6, pp. 1078–1096, Dec. 2020.

[38] X. Xue, K. Zhang, K. C. Tan, L. Feng, J. Wang, G. Chen, X. Zhao, L. Zhang, and J. Yao, "Affine transformation-enhanced multifactorial optimization for heterogeneous problems," *IEEE Trans. Cybern.*, early access, Dec. 15, 2020, doi: 10.1109/TCYB.2020.3036393.

[39] A. Gupta, Y.-S. Ong, L. Feng, and K. C. Tan, "Multiobjective multifactorial optimization in evolutionary multitasking," *IEEE Trans. Cybern.*, vol. 47, no. 7, pp. 1652–1665, Jul. 2017.

[40] N.-Y. Liang, G.-B. Huang, P. Saratchandran, and N. Sundararajan, "A fast and accurate online sequential learning algorithm for feedforward networks," *IEEE Trans. Neural Netw.*, vol. 17, no. 6, pp. 1411–1423, Nov. 2006.

[41] Y. Yuan, Y.-S. Ong, L. Feng, A. K. Qin, A. Gupta, B. Da, Q. Zhang, K. Chen Tan, Y. Jin, and H. Ishibuchi, "Evolutionary multitasking for multiobjective continuous optimization: Benchmark problems, performance metrics and baseline results," 2017, *arXiv:1706.02766*. [Online]. Available: http://arxiv.org/abs/1706.02766

[42] S. Jiang, Y.-S. Ong, J. Zhang, and L. Feng, "Consistencies and contradictions of performance metrics in multiobjective optimization," *IEEE Trans. Cybern.*, vol. 44, no. 12, pp. 2391–2404, Dec. 2014.

[43] X. Liao, Q. Li, X. Yang, W. Zhang, and W. Li, "Multiobjective optimization for crash safety design of vehicles using stepwise regression model," *Struct. Multidisciplinary Optim.*, vol. 35, no. 6, pp. 561–569, Jun. 2008.

[44] K. Dorling, J. Heinrichs, G. G. Messier, and S. Magierowski, "Vehicle routing problems for drone delivery," *IEEE Trans. Syst., Man, Cybern. Syst.*, vol. 47, no. 1, pp. 70–85, Jan. 2017.

[45] B. L. Golden, S. Raghavan, and E. A. Wasil, *The Vehicle Routing Problem: Latest Advances and New Challenges*, vol. 43. Cham, Switzerland: Springer, 2008.

[46] I. Hong, M. Kuby, and A. T. Murray, "A range-restricted recharging station coverage model for drone delivery service planning," *Transp. Res. C, Emerg. Technol.*, vol. 90, pp. 198–212, May 2018.

[47] K. C. Tan, L. H. Lee, Q. L. Zhu, and K. Ou, "Heuristic method for vehicle routing problem with time windows," *Artif. Intell. Eng.*, vol. 15, no. 3, pp. 281–295, 2001.

[48] H. Coxeter, *Introduction to Geometry*. New York, NY, USA: Wiley, 1969.

[49] N. Christofides, A. Mingozzi, and P. Toth, "The vehicle routing problem," in *Combinatorial Optimization*, N. Christofides, N. Mingozzi, A. Toth, and C. Sandi, Eds. Chichester, U.K.: Wiley, 1979.

[50] B. L. Golden, E. A. Wasil, J. P. Kelly, and I. M. Chao, "The impact of metaheuristics on solving the vehicle routing problem: Algorithms, problem sets, and computational results," in *Fleet Management and Logistics*. Boston, MA, USA: Springer, 1998, pp. 33–56.

[51] E. Uchoa, D. Pecin, A. Pessoa, M. Poggi, T. Vidal, and A. Subramanian, "New benchmark instances for the capacitated vehicle routing problem," *Eur. J. Oper. Res.*, vol. 257, no. 3, pp. 845–858, Mar. 2017.

[52] S. Tsutsui and G. Wilson, "Solving capacitated vehicle routing problems using edge histogram based sampling algorithms," in *Proc. Congr. Evol. Comput.*, 2004, pp. 1150–1157.

[53] H. Nazif and L. S. Lee, "Optimised crossover genetic algorithm for capacitated vehicle routing problem," *Appl. Math. Model.*, vol. 36, no. 5, pp. 2110–2117, May 2012.

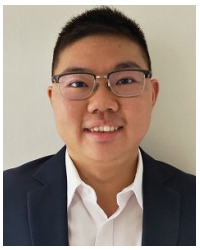

RAY LIM received the B.E. degree in mechanical engineering from Nanyang Technological University, Singapore, in 2015, where he is currently pursuing the Ph.D. degree in computational intelligence from the School of Computer Science and Engineering. His current research focus is in the study of solution representation learning strategies to increase the effectiveness of knowledge transfers across optimization tasks, using probabilistic model-based transfer evolutionary optimization algorithms.

LEI ZHOU received the B.E. degree from the School of Computer Science and Technology, Shandong University, Shandong, China, in 2014, and the Ph.D. degree from the College of Computer Science, Chongqing University, Chongqing, China, in 2019. He is currently a Postdoctoral Research Fellow with the School of Computer Engineering, Nanyang Technological University, Singapore. His current research interests include evolutionary computations, memetic computing, as well as transfer learning and optimization.

ABHISHEK GUPTA (Senior Member, IEEE) received the Ph.D. degree in engineering science from the University of Auckland, New Zealand, in 2014. He currently works as a Scientist and Technical Lead with the Singapore Institute of Manufacturing Technology (SIMTech), Agency for Science, Technology and Research (A∗STAR), Singapore. He has diverse research experience in the field of computational science, ranging from numerical methods in engineering physics, to topics in computational intelligence. His current research interests include intersection of optimization and machine learning, with particular emphasis on probabilistic model-based search algorithms, transfer and multi-task learning. He is an Associate Editor of the IEEE TRANSACTIONS ON EMERGING TOPICS IN COMPUTATIONAL INTELLIGENCE, an Editorial Board member of the *Complex & Intelligent Systems* Journal, *Memetic Computing* Journal, and Co-Editor of the Springer Book Series on Adaptation, Learning, and Optimisation.

YEW-SOON ONG (Fellow, IEEE) received the Ph.D. degree in artificial intelligence in complex design from the University of Southampton, U.K., in 2003. He is currently the President's Chair Professor of computer science with Nanyang Technological University (NTU). He holds the position of Chief Artificial Intelligence Scientist of the Agency for Science, Technology and Research Singapore. At NTU, he works as the Director of the Data Science and Artificial Intelligence Research and the Co-director of the Singtel-NTU Cognitive & Artificial Intelligence Joint Laboratory. His research interests include artificial and computational intelligence. He has received several IEEE outstanding paper awards and was listed as a Thomson Reuters highly cited researcher and among the World's Most Influential Scientific Minds. He is a founding Editor-in-Chief of the IEEE TRANSACTIONS ON EMERGING TOPICS IN COMPUTATIONAL INTELLIGENCE. He is an Associate Editor of the IEEE TRANSACTIONS ON NEURAL NETWORKS & LEARNING SYSTEMS, the IEEE TRANSACTIONS ON CYBERNETICS, the IEEE TRANSACTIONS ON ARTIFICIAL INTELLIGENCE, and others.

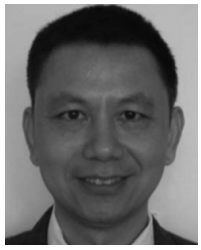

ALLAN N. ZHANG received the Ph.D. degree in artificial intelligence from Wuhan University, Wuhan, China, in 1992. He is currently a Senior Scientist with the Singapore Institute of Manufacturing Technology, A∗STAR, Singapore. He has over 20 years' experiences in knowledge-based systems and enterprise information systems development. His current research interests include knowledge management, data mining, machine learning, artificial intelligence, computer security, software engineering, software development methodology and standard, and enterprise information systems. He and his team are currently involved in the research of manufacturing system analyses including data mining, supply chain information management, supply chain risk management using complex systems approach, multi-objective vehicle routing problems, and urban last mile logistics.